Relationships Among Morphology, Texture, and Chemistry in Stromatolites of the Green River Formation (Eocene, Wyoming, USA)

Reiners, Lindsey

A thesis submitted in partial fulfillment of the requirement of the
Bachelor of Arts
(Geology)
At Gustavus Adolphus College
2017

TABLE OF CONTENTS

Relationships among Morphology, Texture, and Chemistry in Stromatolites of the Green River Formation (Eocene, Wyoming, USA)

By Lindsey Reiners
Under the supervision of Julie K. Bartley

Abstract

Stromatolites are layered, accretionary structures that form by the interaction of sediment and microbes. They are among the earliest records of life on Earth and can be useful in interpreting Earth's past environments. Microbes and sediment interact to construct stromatolites in two fundamental ways: by in situ mineral precipitation and by the trapping and binding of carbonate grains. With these basic building blocks, stromatolites express a wide variety of microscale textures and macroscopic forms that have the potential to record aspects of the environment in which they grew. However, the relationships among their morphology, texture, and chemical environment are poorly understood.

Stromatolites through time are abundant in a variety of marine, and freshwater settings, and in saline to hypersaline conditions. Lakes, especially closed-basin lakes that experience frequent changes in size and salinity, provide a good record of environmental changes because of their sensitivity to precipitation and evaporation. Likewise, the morphology, texture, and chemistry of stromatolites are greatly influenced by environmental changes.

The Green River (Eocene) is a lacustrine carbonate and clastic formation that spans across parts of Wyoming, Colorado, and Utah. To probe connections between morphology, texture, and chemistry, samples were collected from stromatolite-rich rock layers at Sand Butte and White Mountain. Despite stark differences in large-scale morphology, detailed petrography shows the stromatolites of both localities share the same fundamental building blocks. Stromatolites from both localities are dominated by precipitated and grumeaux microscale fabrics, with one subsidiary trapped-and-bound texture. Trace-element analysis using ICP-MS suggested no correlation between stromatolite microstructure and chemistry. However, a potential relationship between individual laminae and chemical composition suggests a lamina can be tracked inward to outward in the Green River stromatolites. This approach, in conjunction with detailed petrography, provided a unique opportunity to establish detailed relationships among texture, morphology, and chemistry for growth mechanisms in stromatolites.

Acknowledgements

I would like to thank Dr. Julie Bartley for invaluable advising; this includes but is not limited to, funding for research through her collaboration with the Petroleum Research Fund, and the constant support and advice on this research topic. I would also like to thank Dr. Laura Triplett, Dr. James Welsh, and Dr. Andrew Haveles of the Gustavus Adolphus Geology Department, for insightful comments and further advising me through the steps of completing this thesis. Further acknowledgments can be extended to Henry Roehler, Paul Buccheim, and Stan Awramik for preparatory fieldwork, including Green River Formation stratigraphy, and stromatolite localities. Dr. Tom Hickson of St.Thomas University, for engaging discussion and collaboration among students and professors on current stromatolite research projects. Former student research also laid important framework for this project, a special thanks to Tanner Eischen, Sydney Firmin, John Berger, and Bailey Hilgren for previous work on Dr. Julie Bartley's stromatolite research team.

Introduction

Stromatolites are not only an early record of life, but also a unique record of the physical and chemical environment in which they grew. They form by a combination of biological activity, physical sedimentation, and changes in water chemistry (Hofmann, 1973). With these components, stromatolites express a wide variety of macroscopic forms, and microscopic textures that host the potential to respond to, and record environmental changes. However, the relationship between these three factors, and the stromatolites preferential growth are poorly understood.

Two basic building blocks are recognized in stromatolites throughout the geologic record. *In situ* mineral precipitation (Fig.1a) is the production of calcium carbonate while the cyanobacteria is actively growing, and can create distinctive layer variations within a stromatolite. The trapping and binding of carbonate grains (Fig.1b) is the second building block recognized in a stromatolite. A unique transition is found within these two building blocks in the geologic record, and is well discussed in Grotzinger and Knoll (1999). Ancient, and more modern lacustrine stromatolites primarily exhibit precipitated textures while modern marine stromatolites, as found in Shark Bay, primarily construct by the

Fig.1. (A) Upward growth by in situ mineral precipitation (B) Stars falling illustrates carbonate grains in trapping and binding.

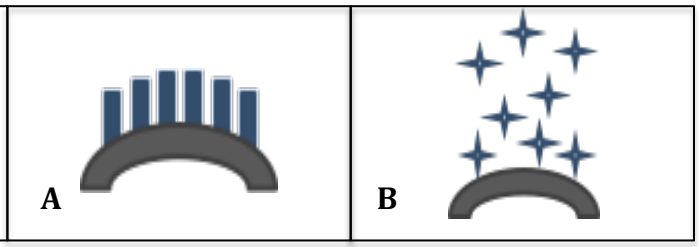

trapping and binding of grains. This transition of growth mechanisms through time limits the use of modern-day analogues, leading to systematic studies to try and reconstruct stromatolite structure, and paleoenvironments.

The mechanisms of growth to produce the distinct similarities of microstructure, and stark differences in large-scale morphology of stromatolites through time are still debated. Hofmann (1973) identified specific criteria for the initiation of growth for stromatolites, and established a systematic way to describe stromatolite morphology and scale in relation to fluxes in their biological, physical, and chemical environment. Riding (2011) reviewed the complex history of stromatolite growth mechanisms through time to establish a common nomenclature to describe stromatolites. In his study, three alternative views of stromatolite microstructure were identified, either biogenic growth, abiogenic growth, or a hybrid of the two. One way to think about these connections in growth mechanisms and across scale, is a bottom to top control model. This means, with specific chemical conditions in the water, biological processes can be initiated, and microstructure would construct biogenically. Hofmann (1973) suggested that macroscale morphology is predominantly a product of physical environment. Bartley et al. (2009, 2015) and Turner et al. (2000) propose that microscale textures are mainly a product of the interaction of

biological processes with carbonate precipitation. Each of the authors speculated that there could be casual connections between these two scales, however previous studies have not investigated these scale connections. Applying this model, a correlation among features at each scale is to be expected.

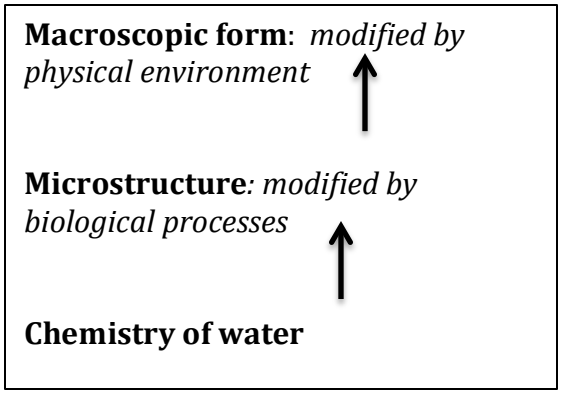

Fig.1c. (*Left*) Illustrates scales of the potential growth model (A) for stromatolites.

The second way to interpret scale connections is using a distinct scale-control model. In this model, each scale would have it's own control, and evidence of all features would be visible in the stromatolite. As the stromatolite grows, the biological processes are controlling the lamina, while the physical environment influences the macroscopic form, and both of these scales potentially record the chemical environment in which they grew.

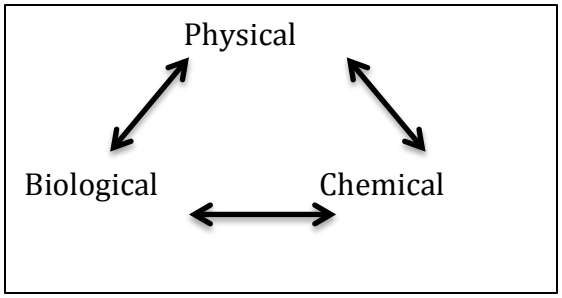

Fig.1d. (*Left*) Illustrates distinct scale controls as a model (B) of growth.

In this work, stromatolites of the Green River formation are analyzed to explore the relationships among geochemistry, microstructure, and morphology to determine whether particular geochemical features are associated with characteristic microstructures, and whether specific combinations of microstructure build particular morphologies. This leads to three primary questions to be asked: are specific morphologies (macrostructures) consistently associated with particular lamina types (microstructures)? Do certain microstructures possess particular geochemical characteristics that suggest a chemical influence on texture development? Can we use this information to describe the physical, chemical, and biological factors that influence stromatolite development?

Geologic Setting

The Green River Formation (Eocene) is a lacustrine deposit that spans across parts of Wyoming, Colorado, and Utah (Roehler, 1973). The formation is primarily a carbonate and clastic unit that contains a wide variety of fossils, including well-preserved lacustrine microbialites. The northern portion of the Greater Green River Basin (Fig.2) corresponds to the maximum extent of Lake Gosiute (Roehler, 1973), a large intermontane lake that existed during the warmest period of the Cenozoic (Smith, Carroll, and Singer, 2008). During this time, the lake went through varying degrees of being connected as one large lake, and disconnected into several basin lakes, as a result of the changing tectonic landscape. This study focused on two stromatolite-rich portions within the Wilkins Peak Member (White Mountain) and Laney Member (Sand Butte).

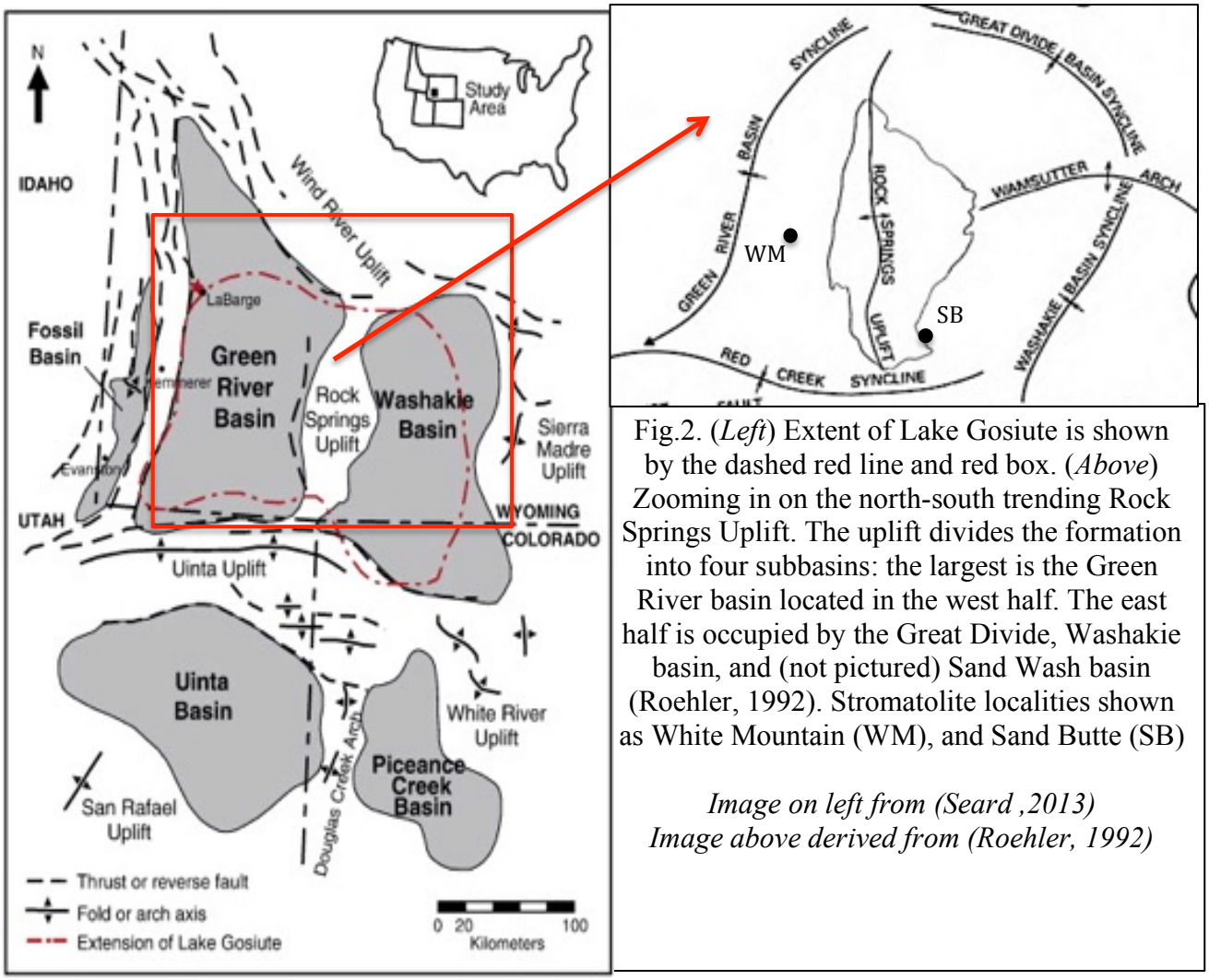

Fig.2. (*Left*) Extent of Lake Gosiute is shown by the dashed red line and red box. (*Above*) Zooming in on the north-south trending Rock Springs Uplift. The uplift divides the formation into four subbasins: the largest is the Green River basin located in the west half. The east half is occupied by the Great Divide, Washakie basin, and (not pictured) Sand Wash basin (Roehler, 1992). Stromatolite localities shown as White Mountain (WM), and Sand Butte (SB)

Image on left from (Seard ,2013)
Image above derived from (Roehler, 1992)

White Mountain, (N41.89371, W109.26606)

The White Mountain outcrop is located in the Green River Basin, near the White Mountain Petroglyphs, north of Rock Springs, Wyoming (Fig. 2, WM). There is a clear contact at this locality between the top of the Tipton (oolitic limestone, shale and clay) and the base of Wilkins Peak (fossiliferous grainstone, or coquina). The Wilkins Peak member consists of carbonate-rich lacustrine deposits that represent a period of lowstand Lake Gosiute (Surdam and Stanley, 1979). Stromatolites were primarily collected in float, with only one horizon in place (Fig.3). However, all stromatolites likely came from the prominent bench at the top of the butte (yellow line in Fig.3).

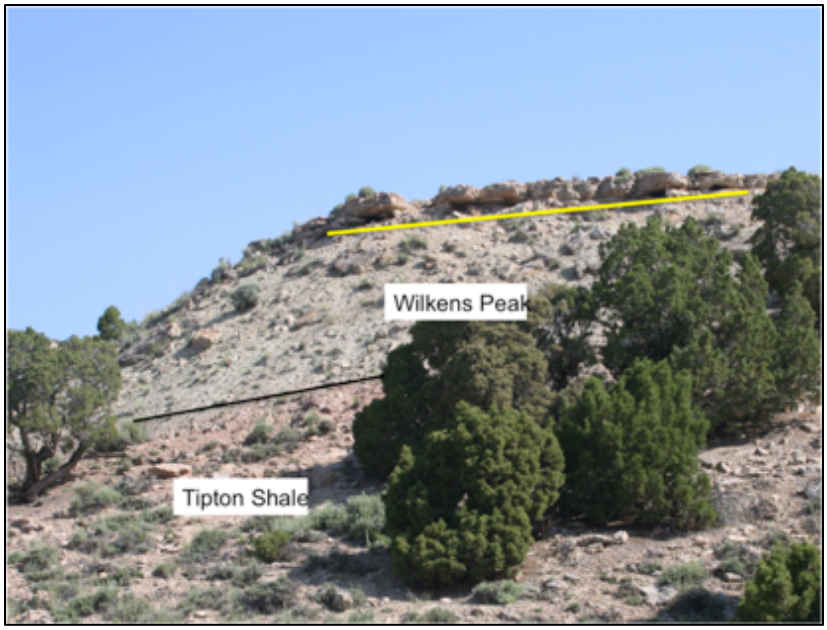

Fig.3. (*Left*) An outcrop photo of White Mountain, the black line indicates approximate contact between the (pink color) Tipton and the (grey color) Wilkins Peak. Yellow underline indicates the resistant bed containing in place stromatolites.

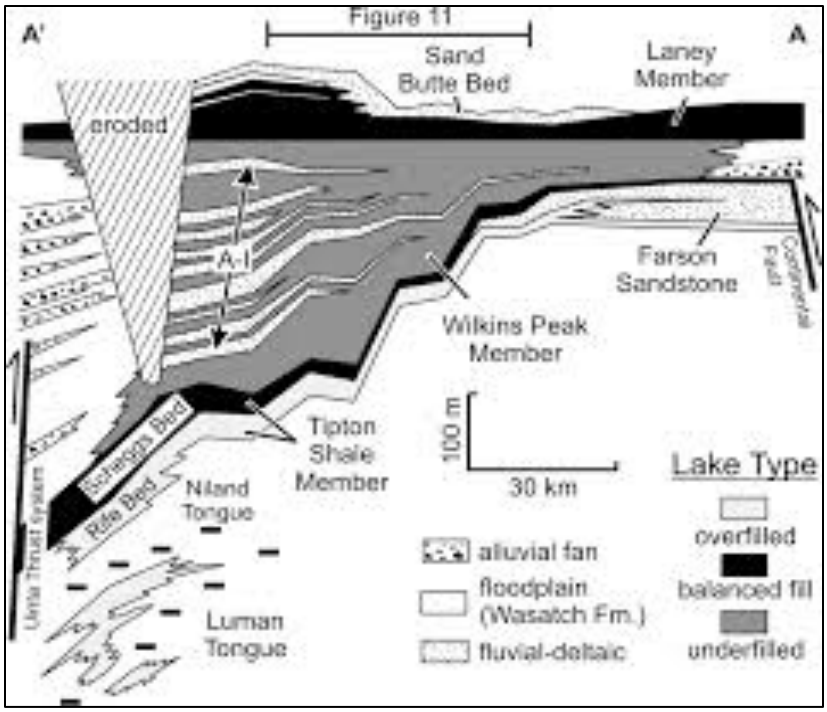

Fig.4. (*Left*) Basin cross section illustrating stratigraphic relationship between Wilkins Peak and Laney Member.

(Pietras, Carroll, 2006)

Sand Butte, (N41.34908, W109.266606)

Sand Butte is located in the Washakie Basin in Sweetwater County, Wyoming (Fig.1, SB). The red fluvial sandstone at the base of the butte is recognized as the Wasatch, followed by the Wilkins Peak, and then the Laney Member. Stromatolites were primarily collected from the Laney member (Laclede Bed), which is recognized as the final transition from saline to freshwater lake.

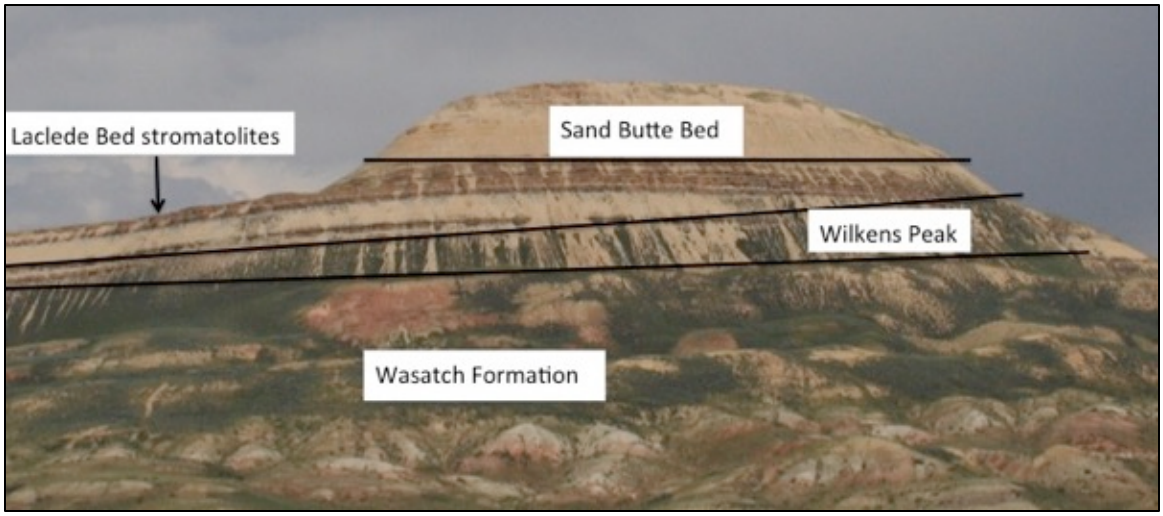

Fig.5. Large-scale outcrop view of Sand Butte and its associated units, the arrow points to horizon stromatolites were primarily sampled and the black lines indicate approximate contacts.

Methods

Stromatolite Nomenclature

There are various scales at which a stromatolite can be described both in the field, and in the laboratory. The macroscopic form is visible at outcrop or hand sample scale and is determined by the curvature, synoptic relief, and inheritance of the laminae in a stromatolite. Synoptic relief is the height of laminae off the seafloor during growth, while inheritance is the degree to which laminae stack on top of one another. Examples of macroscopic forms found in the Green River Formation are in figure 6, the nomenclature is as follows: domal (c), columnar (d), and stratiform (e).

Zooming in, the microstructure is the petrographic characteristics of individual laminae. These microstructures build laminae, and are known as the basic building blocks of stromatolites. Within the primary building blocks, stromatolites can also express various fabrics. In situ mineral precipitation produces fabrics that allow stromatolites to build steep laminae, with high inheritance since the microbial mat is partially lithified from precipitation. At the same time, parts of the microbial mat can begin decay and

create interesting clots in the fabric. Examples of two common precipitated fabrics are isopachous, and grumeaux (decaying texture) (Fig.8). Trapping and binding texture follows the law of gravity, and tends to have a more clastic fabric. Subsidiary trapped and bound textures can be observed within some of the Green River stromatolites, within this fabric, ostracods are visible along the relief of the laminae.

Fieldwork and collection

Field research was conducted in the summer of 2015 with the goal of collecting a diverse selection of microbialites from across both time and space. Samples were collected from stromatolite-rich horizons at White Mountain (Greater Green River Basin) and Sand Butte (Washakie Basin). To explore the relationship between texture, morphology, and chemistry, the criteria for sampling was based on macroscale morphology type and stratigraphic placement. Detailed sections were measured using a Jacob staff and level sight. The microbialites were found in well-exposed outcrops, with samples collected both in place and in float. Images were taken at each site before and after the sample was collected to preserve stratigraphic context. Samples were clearly labeled, and bagged according to locality and geologic unit.

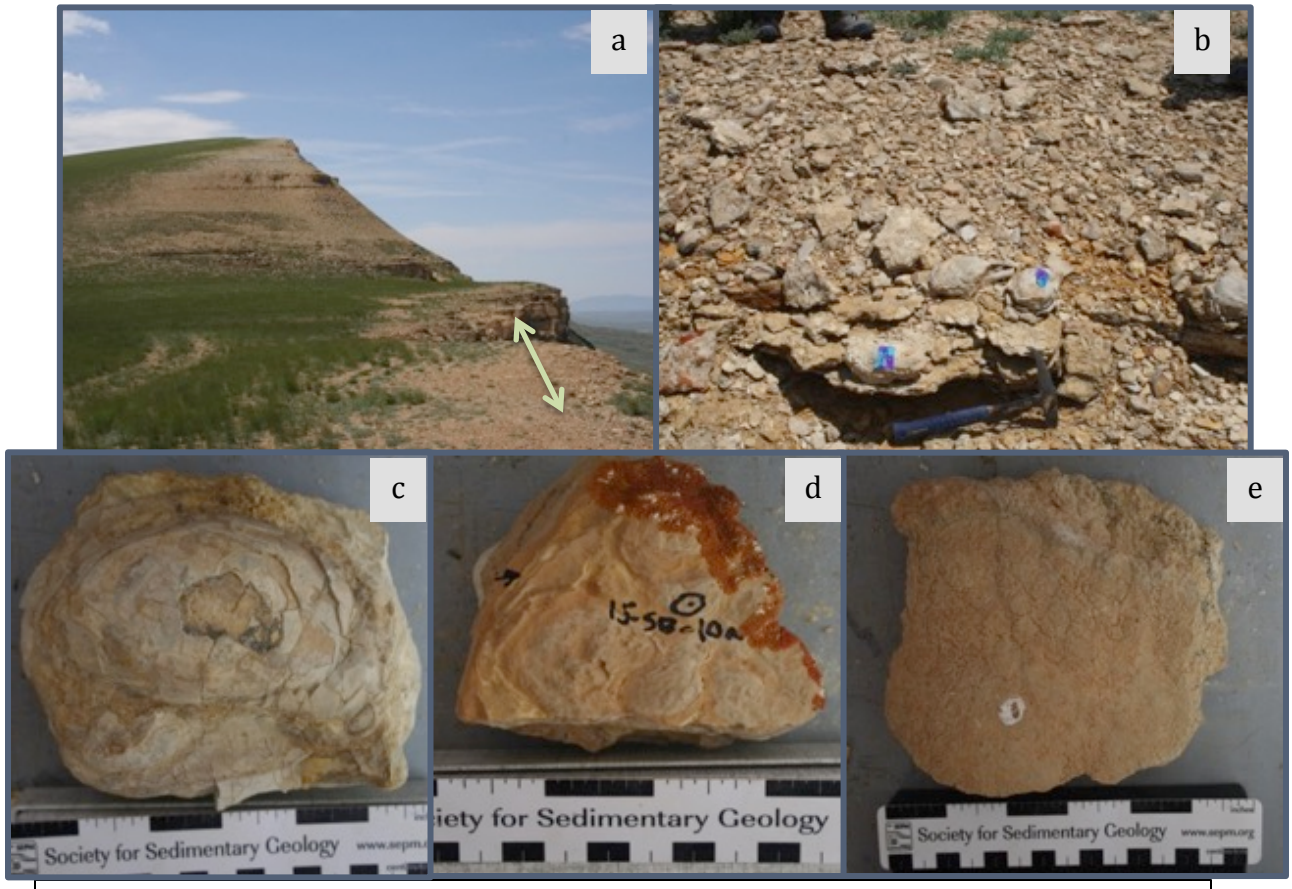

Fig.6. From outcrop to hand sample: Examples of the stromatolites of Sand Butte and method of collection. (*a*) Sand Butte locality with arrow pointing to stromatolitic horizon. (*b*) Bioherm on Sand Butte showing method of sampling. (*c,d,e*) Examples of various stromatolite morphologies collected from a single stratigraphic level, from left to right, domal, colloform, stratiform type. (Laclede Bed, Sand Butte).

Petrographic procedures

Microbialites were impregnated with Epothin epoxy prior to cutting to stabilize the sample, and preserve texture and continuity in laminations. Small samples were cut using a water-cooled rock saw, while larger samples were cut using a mineral oil rock saw. Billets were cut for both large format (75x50mm) and small format (46x27mm) thin sections and polished using levels 120 to 600 grit on an electric buffer. Completed billets were sent to Precimat to be thin sectioned as a 130mm thick covered section. Detailed petrography was performed using cathodoluminescence on polished billets and plain light microscopy on thin sections to identify carbonate and microbial fabrics.

ICP-MS analysis procedure

The Green River stromatolites are characterized by mm-scale to cm-scale light and dark laminations that represent different microfabrics. Stromatolites from a single stratigraphic horizon (Laclede Bed, Laney Member) were microdrilled according to texture and lamination frequency (Fig.8). One complex bioherm from White Mountain (Rife Bed, Wilkins Peak Member) was drilled by following individual laminae, base to top, through each herm (Fig.7 and 13). To precisely drill the targeted fabric, drilling was done using a Servo auto sampler with a 1mm dental carbide bit. Each drill point was no more than 2mm in depth to avoid drilling into an unseen fabric in the 3-D structure. Approximately 1mg of powder was collected from a set of drill points, and placed into sterile falcon tubes. The powdered samples were dissolved using a standard carbonate dissolution procedure (*appendix I*). Major, trace, and rare earth element concentrations were measured on an Agilent 7500 series ICP-MS.

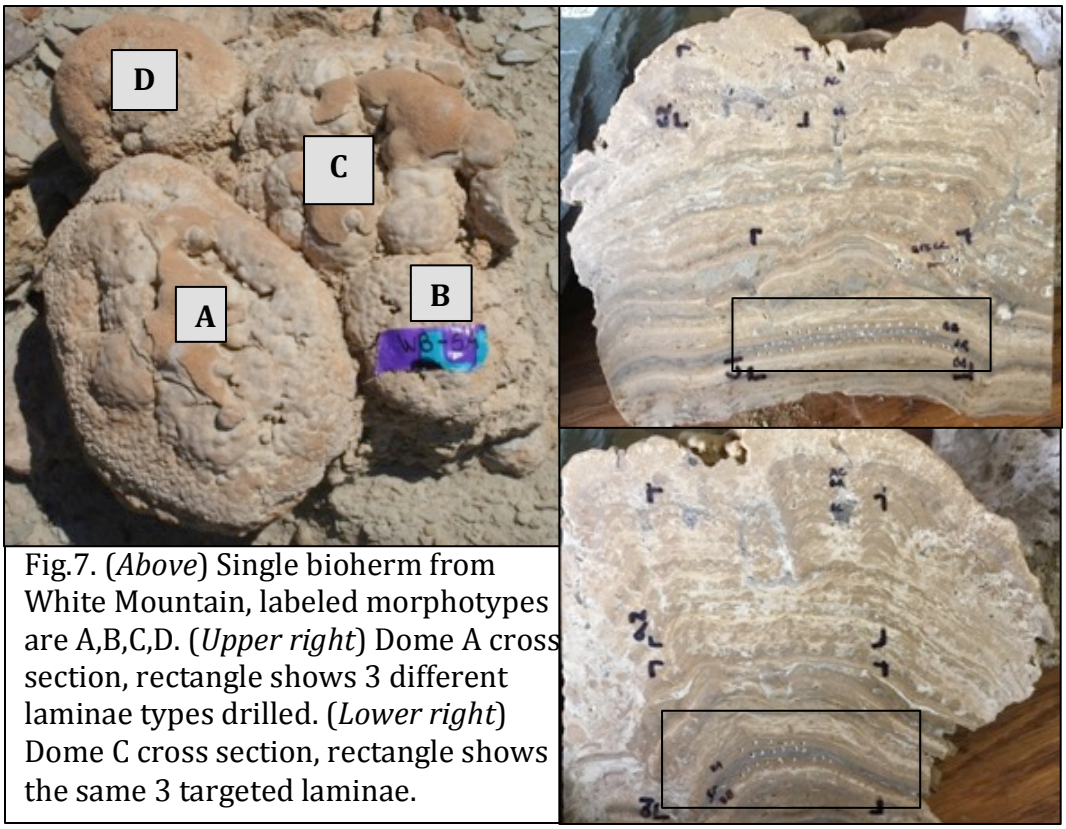

Fig.7. (*Above*) Single bioherm from White Mountain, labeled morphotypes are A,B,C,D. (*Upper right*) Dome A cross section, rectangle shows 3 different laminae types drilled. (*Lower right*) Dome C cross section, rectangle shows the same 3 targeted laminae.

Results

Sand Butte Petrography: Probing morphology and texture

The macroscopic form of the Laney member stromatolites varied across a single stratigraphic horizon. Well-preserved domal, colloform, and stratiform morphology types can be found within this member (Fig.8). On the cut face, the stromatolites display exceptionally preserved microstructures that can be seen with a plain eye (Fig.8). At hand sample, stratiform, crinkly laminae branch into digitate columns within the stratiform and colloform samples. From center to the top of the domal sample, laminae inheritance can be seen increasing, with the highest inheritance along the outer crust. Detailed petrography of the various microstructures clarified the dominant carbonate microfabric. Each morphology type displays multiple types of microstructures, the five main types were isopachous, a silica-rich texture, micrite, grumeaux, and an unlaminated portion.

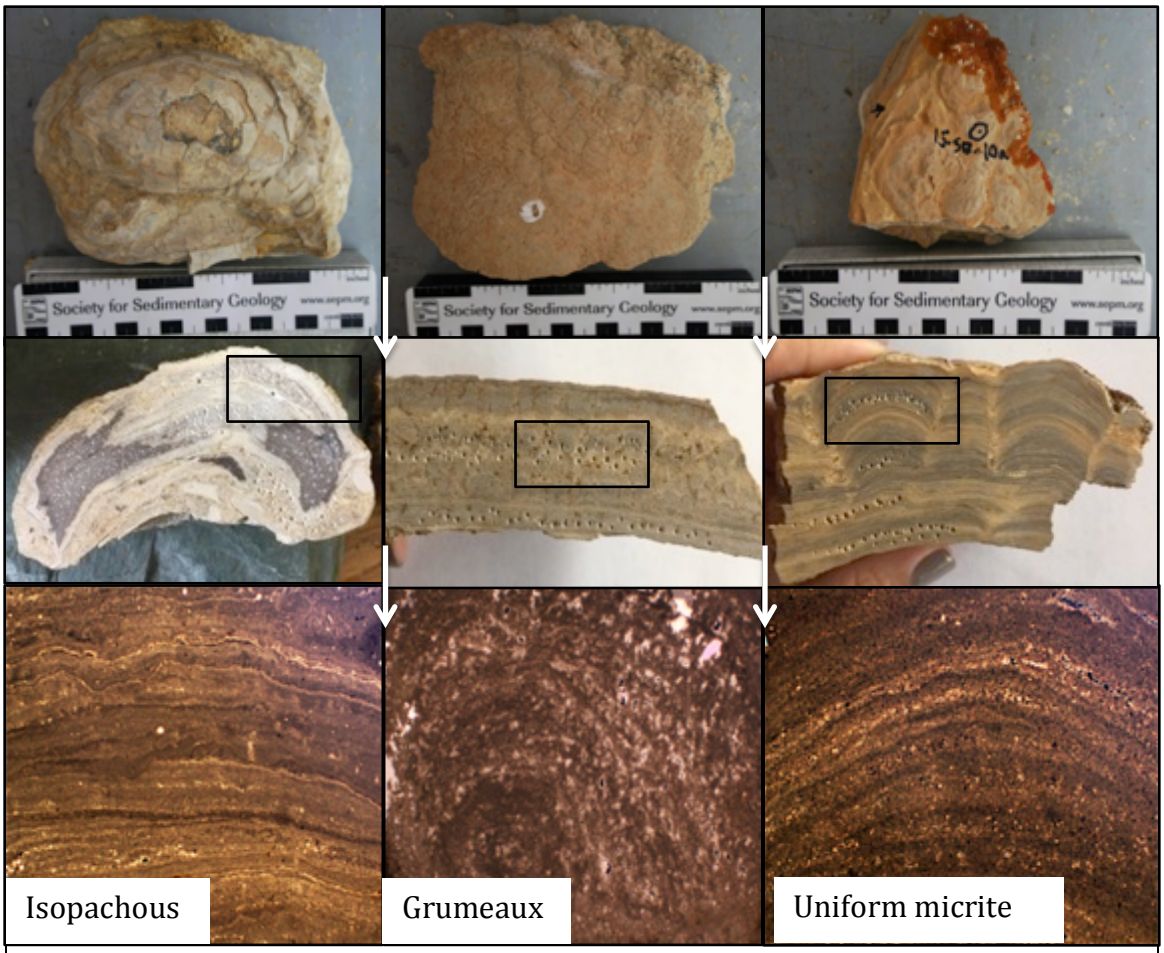

Fig.8. From hand sample to microstructure. Black box (middle row) represent where the microscope image is located on the stromatolite. In this example, a different microstructure is shown in each sample, however, all samples contain multiple types of microstructures.

ICP-MS results

Elemental concentrations were calculated using a formula (*end of appendix 1*) that assumes trace element substitution into the carbonate lattice. Using excel, major, trace, and rare earth elements were initially graphed against a major element as a constant based on microstructure-type for each stromatolite. This organized the data to more clearly represent any trends. Raw data tables can be found in appendix II.

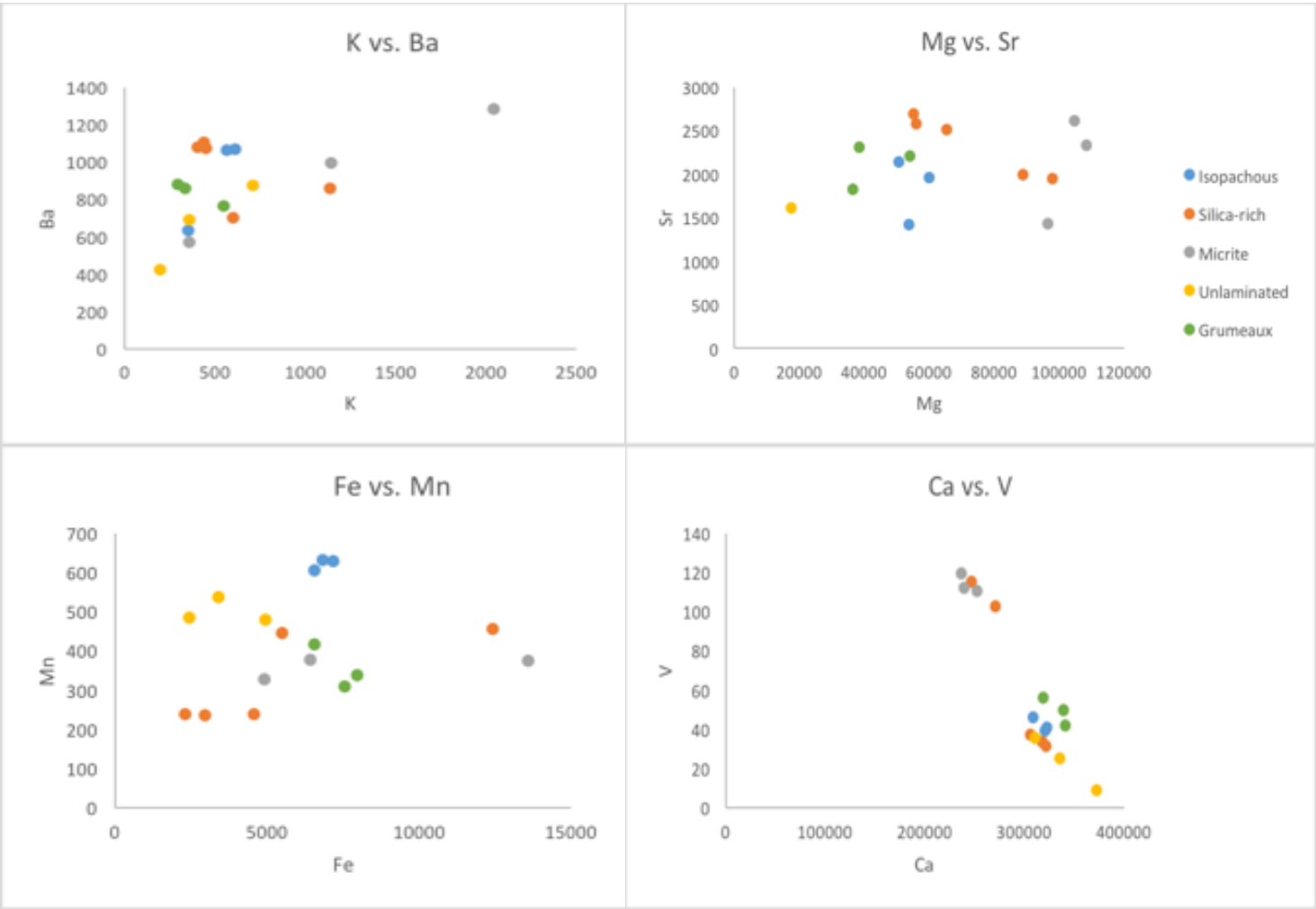

Fig.9. Select scatterplots depicting microstructure type by color, (ppm). Legend on right lists precipitated microstructures: (top) isopachous, silica-rich, micrite, unlaminated, and grumeaux (bottom).

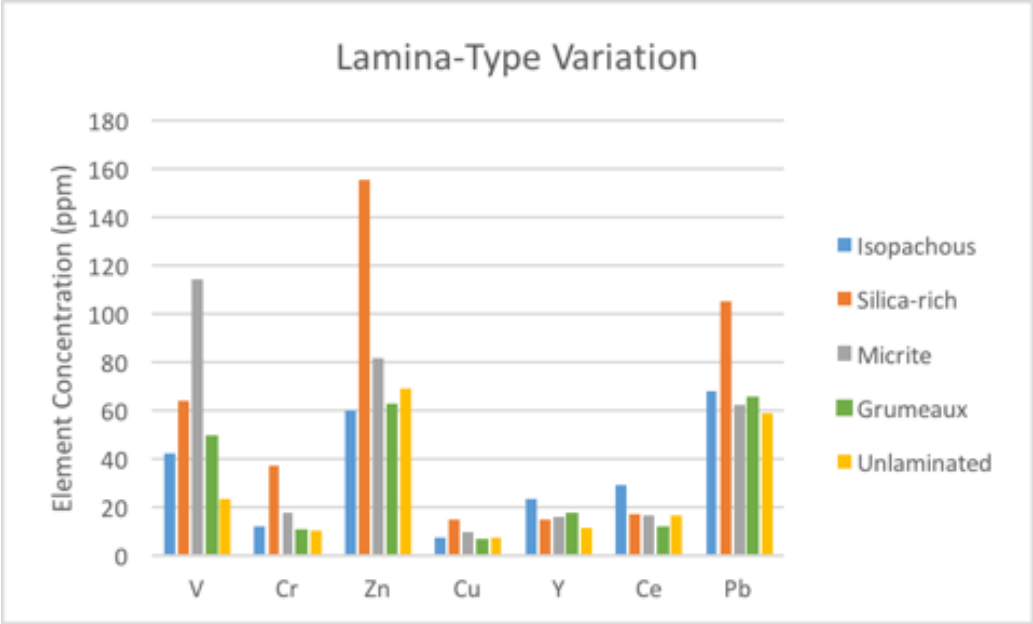

Fig.10. Bar chart representing elemental concentration (ppm) for each microstructure listed in figure 9.

In a previous study, Frantz et al. (2014) noted a systematic change in Na concentration in Green River stromatolites and suggested that patterns in Na-concentration might be related to degree of evaporation during growth. Similarly, Uranium has the ability to track chemical signals.

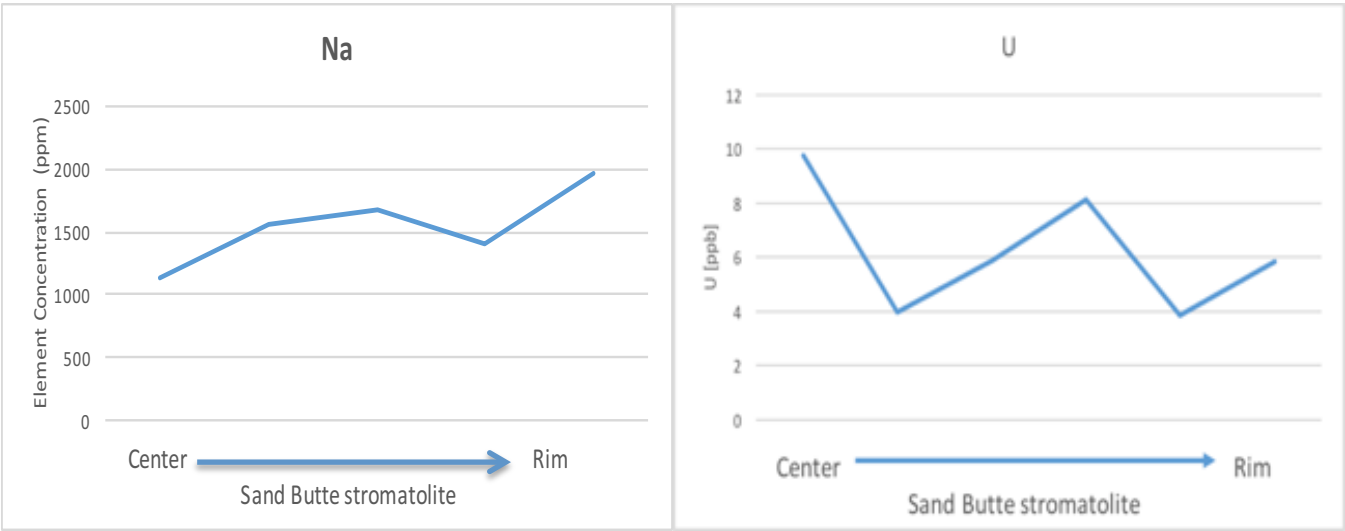

Fig.11. Graph illustrating sodium concentration, from center to rim in domal sample.

White Mountain Petrography: Probing morphology and texture

The Wilkins Peak member stromatolite consisted of four, inter-connected bioherms that varied in macroscopic morphology. Dome A displays a domal macroscopic form with a faint colloform structure in the center. Dome B and D are smaller, smooth domal structures. Dome C has a distinct colloform macrostructure (Fig.7). The cut face displays well-persevered low-relief laminations on the lower half of all domes, and digitate columns branching on the upper half (Fig.13). The microstructures were primarily grumeaux, and uniform micrite with some laminae having a small degree of isopachous layering.

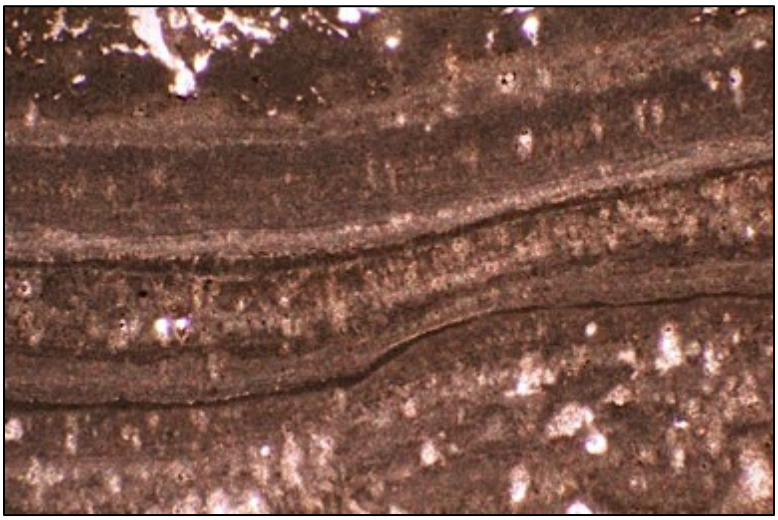

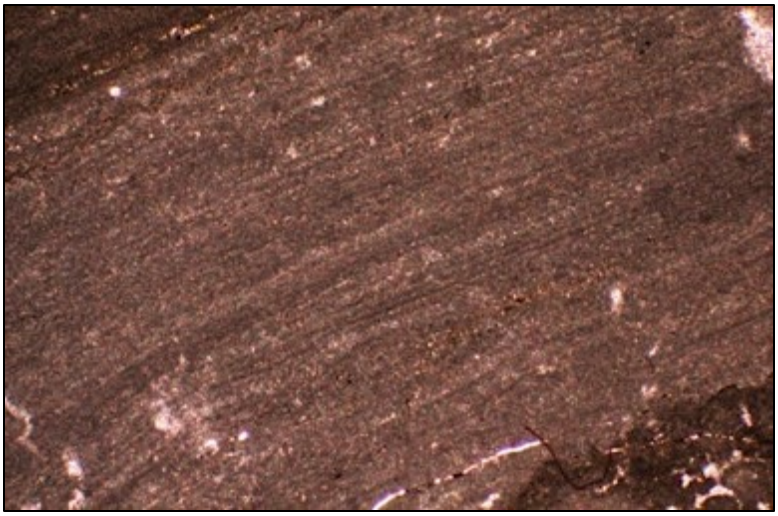

Fig.12. (*Top*) Thin section image of dome A, a degree of upward growth can be seen in the micritic fabric.

Long axis: 2 mm

(*Below*) Uniform micrite fabric in dome A showing small degree of isopachous layering.

ICP-MS results

The image below represents the targeted laminae within one of the domes on the White Mountain stromatolite. The laminae were drilled from base to top, assuming each laminae represents a point in time within the stromatolites growth span.

Figure 13

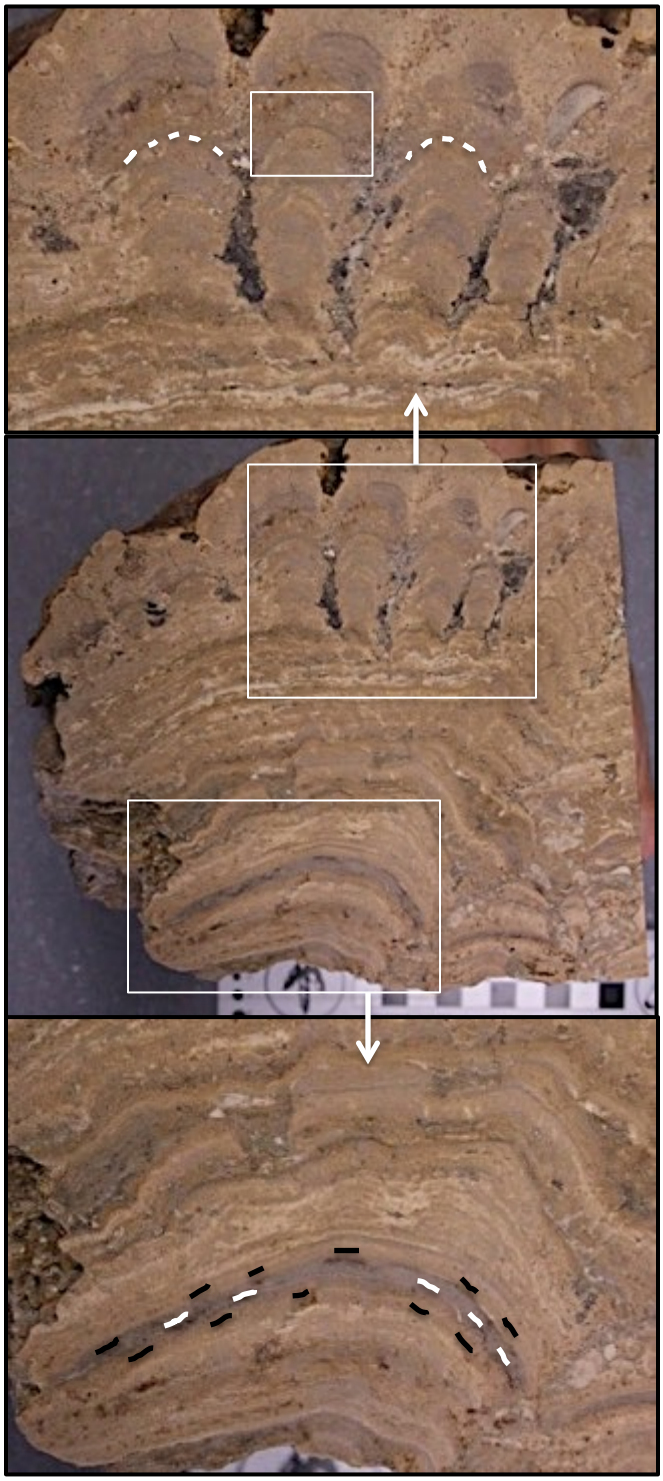

(Upper Left) The white dashes represent the lamina tracked through the columns. The lamina 4 was drilled directly below the white dash, and the lamina 5 was drilled directly above the white dashes.

(Middle Left) Example of the cut face of a dome in the White Mountain stromatolite. White boxes indicate targeted lamina for drilling.

(Lower Left) The black dashed lines below the white dashes mark the location of lamina 1. The white dashes represent lamina 2, and the black dashes above represent lamina 3.

Elemental concentrations were determined using the same procedure as the Sand Butte stromatolites. Each lamina was graphed on a crossplot using a major element as a constant to bring out any trends (Fig.14). The colors represent each lamina within each of the four domes.

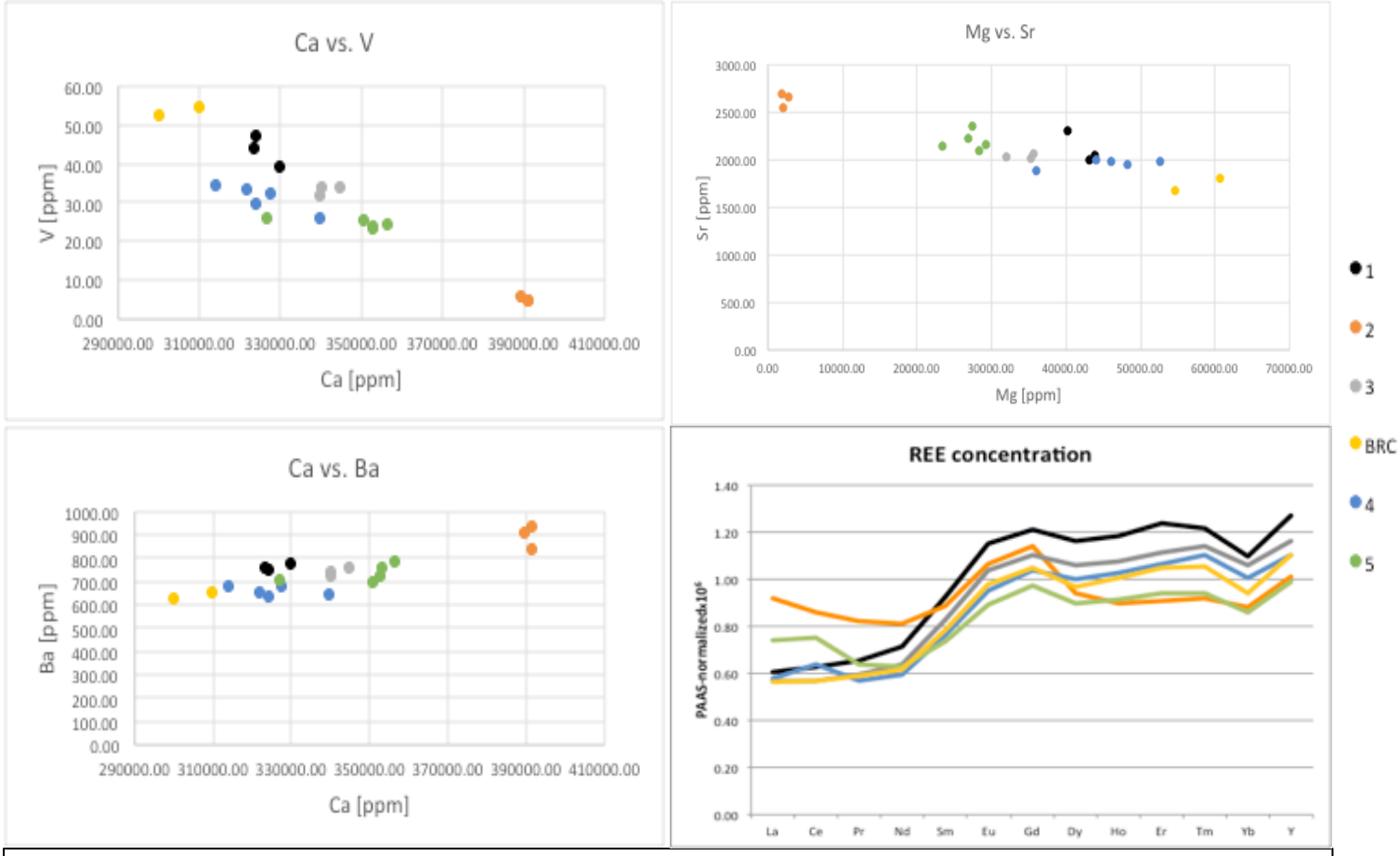

Fig.14. Scatterplots illustrating relationship between laminae and chemistry. The grouping of colors represents the same lamina growing at the same time through all four domes. 1 being the base of the stromatolite, and lowermost lamina drilled, legend is moving to the top of the stromatolite with 5 being the uppermost lamina. BRC is an isolated brecciated texture found in two of the herms.

Discussion

Relationships among morphology type, microstructure, and geochemistry

Despite the stark differences in macroscopic form, nearly all Green River stromatolites from both localities observed are constructed by *in situ* mineral precipitation, with one exception of a silica-rich, subsidiary trapped-and-bound texture. Each morphology type also hosted multiple microstructure fabrics. This suggests microstructure is not well-predicted by macroscale-type, and the two would act independently of each other. Leading to the next question probed, is there a relationship

between microstructure-type and the environment in which they grew (ionic content in water)? ICP-MS results show no distinct correlation within the crossplots of elemental concentration (Fig.9). The zoning of colors do not follow any trend, and concentrations vary within one microstructure type. The bar chart (Fig.10) represents the concentration of a set of elements, each microstructure shares a similar concentration across the chart, further suggesting microstructure is not well-predicted by its water chemistry.

The slight fluctuations seen in the graphs in figure 11 suggest laminae in a stromatolite have a distinct chemical signal, perhaps allowing the lamina to be tracked through time. The graphs in figure 14 shows distinct grouping of data points (by color), with each color representing a specific lamina. The grouping of colors suggests the same laminae through the four domes share similar chemical compositions. This potentially points to lamina-by-lamina trends (similar to Frantz et al., 2014) that will hopefully give further insight into the relationship between stromatolite growth and fluctuations in chemical environment. However, the grouping of data points are not organized linearly (base to top), suggesting the stromatolite is not systematically recording changes within the environment. Laminae holding distinct chemical signals would also describe the unreliability of using geochemistry to predict microstructures, since the microstructure is essentially a cluster of laminae constructing.

Similarities in stromatolite structural components across time and space suggest that the mechanisms of microbialite construction are broadly comparable in many settings, pointing to a potential relationship between geochemistry, morphology, and texture. However, these scales seem to operate more independently than previously suggested (Hofmann, 1973; Grotzinger and Knoll, 1999). Hofmann suggested that macroscale morphology is predominantly a product of physical environment. Bartley et al. (2009, 2015) and Turner et al. (2000) propose that microscale textures are mainly a product of the interaction of biological processes with carbonate precipitation. Geochemical data collected in this study suggests that the trace element composition has little to no influence on either the stromatolite's texture or morphology. The ternary diagram on the right illustrates the distinct scale control model (B). In this model, the stromatolite displays a mosaic of features, with evidence of the chemical environment in both the microstructure, and macrostructure.

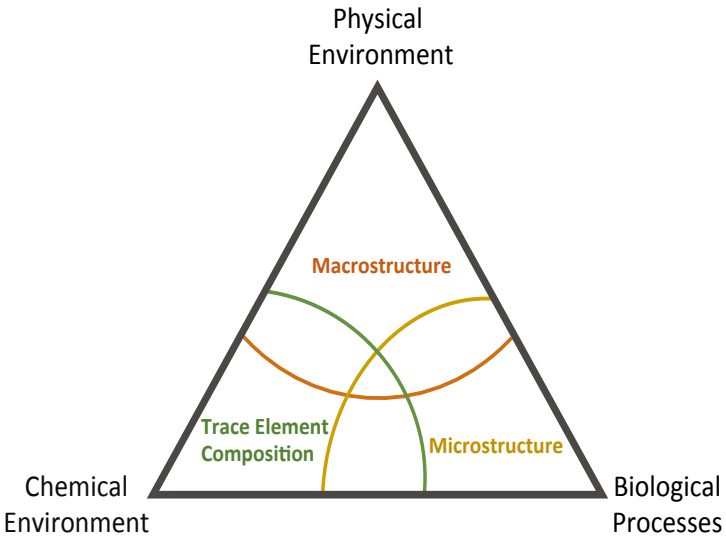

Figure modified from Hofmann (1973)

References

Awramik, S., Buccheim, P., 2015, Giant stromatolites of the Eocene Green River Formation (Colorado, USA): Geology [Boulder], v.40, p. 691-694.

Bartley, J.K, Kah, L.C, Frank, T.D, Lyons T.W, 2015, Deep-water microbialites of the Mesoproterozoic Dismal Lakes Group: microbial growth, lithification, and implications for coniform stromatolites: Geobiology v.13, p.15-32.

Frantz, Carie M., Petryshyn, Victoria A., Marenco, Pedro J., Tripati, Aradhna, Berelson, William M., Corsetti, Frank A., Dramatic local environmental change during the Early Eocene Climatic Optimum detected using high resolution chemical analyses of Green River Formation stromatolites: Palaeogeography, Palaeoclimatology, Palaeoecology (2014), doi: 10.1016/j.palaeo.2014.04.001

Grotzinger, J.P., Knoll, A.H., Stromatolites in Precambrian Carbonates: Evolutionary Mileposts or Environmental Dipsticks? Annual Review of Earth and Planetary Sciences, v.27, p.313-358.

Hofmann, H. 1973, Stromatolites: characteristics and utility: Earth Science Reviews, v. 9, p.339-373.

Leggitt, L., Biaggi, E., Buccheim, P., 2007, Palaeoenvironments associated with caddisfly-dominated microbial-carbonate mounds from the Tipton Shale Member of the Green River Formation: Eocene Lake Gosiute: Sedimentology, 51, p.661-699.

Pietras, J., Carroll, A., 2006, High-Resolution stratigraphy of an underfilled lake basin: Wilkins Peak Member, Eocene Green River Formation, Wyoming, U.S.A: Journal of Sedimentary Research, v.76, p.1197-1214.

Riding, R., 2011, The Nature of Stromatolites: 3,500 Million Years of History and a Centur of Research, Advances in Stromatolite: Geobiology, v.131, p.29-74.

Roehler, H., 1973, Stratigraphic divisions and geologic history of the Laney Member of the Green River Formation in the Washakie Basin in southwestern Wyoming, U.S Geological Survey professional paper, p. 1-34.

Roehler, H., 1992, Introduction to greater Green River Basin geology, physiogeography, and history of investigations, U.S Geological Survey professional paper, p.1-19.

Seard, C., Camoin, G., Rouchy, J.M., Virgone, A., 2013, Composition, structure and evolution of a lacustrine carbonate margin dominated by microbialites: Case study from the Green River formation (Eocene; Wyoming, USA): Paleogeography, Paleoclimatology, Palaeoecology, v.381-382, p.128-144.

Smith, E., Carroll, A., Singer, B., 2008, Synoptic reconstruction of a major ancient lake system: Eocene Green River Formation, western United States, GSA bulletin, v.120, p. 54-84.

Appendix

I. Carbonate Dissolution

Procedure- Carbonate Dissolution for ICP-MS

1. Weigh sample into a 15 mL "Falcon" tube, w/ conical end for centrifugation
   a. If you're only interested in major and significant trace elements (Ca, Mg, Fe, Mn, Sr), 0.25 mg (0.0025 g) is sufficient. If you are interested in low-abundance elements (e.g., REE), use 0.5-1.5 mg. On an ICP-MS, you should avoid using more than 6 mg, because the total dissolved solids load becomes too high and the instrument's cones clog.
   b. Record weight – the mass is *not* used to calculate final concentrations for carbonate*; however, we frequently use the mass to determine whether ICP-MS values obtained are sensible.
      *Note: The calculation of elemental concentrations assumes that all dissolved mineral phases are carbonate (calcite + dolomite) and uses the stoichiometric relationship for carbonates to compute concentrations. If you think your mineralogy is unusual, you might want to measure mass directly and compute concentration from rock mass. If this is the case, record (1) mass of empty 15 mL tube; (2) mass of dry powder; (3) mass of dried insoluble residue (dry the first tube after step 6 and record mass of insoluble residue); (4) total acid volume in ICP (volume [or mass] transferred to clean tube + volume [or mass] added).
2. Add ~2 mL 2% trace metal grade (TM) spiked (w/ 100 ppb internal standard) HNO_3
   a. Recipe for 1 L of 2% spiked nitric acid: (1) put some (maybe 500 mL or so) milli-Q water in a 1000 mL volumetric flask. Add 28.5 mL concentrated, trace-metal grade HNO_3 + 10.0 mL internal standard then add milli-Q grade water to fill volumetric to exactly 1000 mL. Transfer to a labeled Nalgene bottle.
   b. Our internal standard consists of Be, Bi, [Ga]*, In, Sc, Tb (100 µg/mL). Ordered from Inorganic Ventures; custom mix name GAC-1. *Note: We stopped using Ga as a reference standard because Inorganic Venture's trace element standards were Ga-contaminated.
3. Mix by vortexing for a few seconds.
4. Let reaction proceed for at least 30 min and as long as overnight.
5. Centrifuge 3 min at 500 rpm (longer and/or faster is OK too)
   a. When using the centrifuge, make sure the weight is equally distributed radially. Get opposite tube pairs equal in weight using the scale and adding additional HNO_3 if necessary.
6. Decant or pipet liquid into clean, labeled ICP tube. The idea is to remove any particulate matter, so that it does not foul the ICP-MS uptake tube.
7. Add enough HNO_3 to make 10 mL. Because we are not using total sample mass to calculate elements for carbonate, it is not necessary to precisely measure the acid (but see note in 1b).
8. Cap and shake. Leave covered (caps on) until ready to run on ICP-MS.

Determine concentrations on ICP-MS, then use the following equation to calculate rock concentration:

$$[M_{rock}] = \frac{[M_{aq}]*400435-(85475*[Mg_{aq}]/[Ca_{aq}])}{\text{Sum [All Elements}_{aq}]}$$

Make sure units for all elements are the same (ppb or ppm), or convert in your spreadsheet.

Table 1: Stromatolite Frequency table at Sand Butte and White Mountain localities

Morphotype	Domal	Colloform	Stratiform	Other
Sand Butte	7	3	2	3
White Mountain	6	11	2	12

II. Raw ICP-MS concentrations

ample Numb	[Mg/Ca]	Sum ppb	23 Na. [ppm	24 Mg. [ppb]	39 K. [ppb]	43 Ca. [ppb]	51 V. [ppb]	52 Cr. [ppb	54 Fe. [ppb]	55 Mn [ppb]	64 Zn [ppb]	65 Cu [ppb]	85 Rb[ppb]	88 Sr [ppb]	89 Y [ppb]	95 Mo [ppb]	137 Ba[ppb]
15SB-11F-2	0.106761	56245.84	1807.1	36441.3	545.5	341333.8	41.84	10.09	7949.0	337.34	91.41	9.42	2.02	1826.13	13.06	4.20	767.00
15SB-11F-3	0.169592	52173.74	1883.2	54146.8	331.0	319277.5	56.33	11.39	6561.5	417.01	49.36	5.76	1.03	2213.24	18.96	3.59	860.51
15SB-7B-4	0.089993	29526.81	1553.4	31626.5	369.2	351433.0	18.47	11.38	4755.0	416.05	115.07	11.33	0.74	1707.78	15.26	4.76	564.46
15SB-7B-5	0.135631	38718.28	1666.5	44982.1	493.6	331650.7	28.54	8.53	6810.2	595.49	55.58	6.30	2.35	1635.06	18.06	2.75	766.04
15SB-9B-1	0.349761	29313.8	2457.8	93089.4	694.6	266151.9	88.01	15.72	4626.8	386.79	55.44	7.05	1.17	1875.46	11.60	4.15	954.55
15SB-9B-2	0.431395	39712.86	3370.8	105149.8	673.2	243743.6	106.48	19.35	6848.4	410.08	82.74	9.22	1.97	2104.61	21.22	3.87	832.97
15SB-9B-3	0.462737	52799.95	1844.6	111420.2	337.7	240785.1	59.33	9.58	3784.1	134.87	32.45	3.72	1.32	1824.29	1.19	1.79	602.42
15SB-10A-1	0.350773	41133.97	2294.4	90518.9	838.4	258055.3	105.75	21.90	15467.2	508.49	87.06	8.61	2.31	1610.63	20.94	3.23	743.39
15SB-10A-2	0.38346	45420.01	2033.8	95863.3	828.2	249995.5	120.35	21.75	15772.3	452.16	42.00	5.32	2.36	1619.79	21.86	2.03	762.15
15SB-10A-3	0.312131	48371.47	2392.4	83027.7	1435.4	266002.6	95.09	19.19	17757.5	521.23	74.17	9.29	3.04	1562.47	22.25	2.18	686.55
15SB-10A-4	0.237466	22694.9	2475.6	69043.8	1291.7	290752.1	83.89	39.13	13361.6	464.17	174.87	17.17	2.56	1565.94	17.08	7.12	612.45
15SB-11A-1	0.409151	66607.48	2059.2	101616.3	502.9	248358.7	106.72	15.77	9801.6	278.95	57.30	5.31	1.93	1782.23	16.36	1.81	764.50
15SB-11A-2	0.382069	49046.73	1705.9	96628.0	353.3	252907.0	110.55	13.96	13566.3	375.34	26.95	4.30	1.47	1429.46	14.65	1.22	570.98
15SB-11F-1	0.113491	59110.71	1435.8	38497.9	293.5	339213.8	49.67	9.78	7561.5	309.83	47.51	5.16	1.07	2311.61	19.56	1.59	878.12
15SB-5A-2	0.161222	19188.61	3368.2	51872.9	836.5	321748.3	26.66	28.85	5009.3	559.18	252.34	23.75	2.25	1723.68	14.87	6.94	869.28
15SB-7A-1	0.17205	18503.87	1863.0	55304.5	436.2	321443.8	31.31	14.07	2289.9	239.68	120.30	15.35	0.50	2689.55	12.37	4.16	1105.07
15SB-7A-2	0.133929	49195.11	1064.0	45010.1	356.2	336073.4	25.04	7.21	3384.7	538.39	30.42	5.57	1.56	1710.77	10.74	1.36	692.71
15SB-7A-3	0.186443	26976.32	2586.3	58687.6	616.4	314775.1	32.40	19.29	3892.8	468.97	207.78	21.01	1.83	2003.48	12.56	5.39	908.94
15SB-7A-1*	0.213576	21109.44	2495.7	65448.5	445.5	306441.2	37.28	63.03	2945.4	235.20	201.47	17.92	0.64	2515.94	12.52	5.98	1072.71
15SB-7A-2*	0.176417	18657.64	1784.3	56136.5	399.7	318203.7	33.50	14.55	4582.3	239.55	121.16	10.02	0.63	2576.55	13.42	3.52	1078.15
15SB-7A-3*	0.21303	36255.54	1488.4	65496.9	349.4	307453.2	38.71	11.69	3455.8	237.40	57.36	9.63	1.05	2436.71	15.30	1.99	1068.84
15SB-7A-4*	0.181472	33262.7	1715.3	57610.6	352.1	317463.4	37.21	13.34	3820.3	316.04	91.06	9.97	1.00	2342.77	11.94	2.74	1007.87
15SB-7A-5*	0.197447	54527.69	2012.2	61385.0	707.3	310894.3	35.72	17.05	4934.9	478.66	108.45	12.26	2.87	1922.31	13.47	3.11	874.21
15SB-7B-1	0.157169	66815.97	1963.9	50765.4	563.7	322998.4	41.01	12.86	6551.8	606.73	71.88	7.73	2.53	2139.10	28.36	2.05	1064.17
15SB-7B-2	0.168071	62810.82	1404.7	53897.4	347.6	320681.3	39.21	9.22	6830.8	631.42	35.14	4.41	0.83	1423.24	17.11	1.43	633.98
15SB-7B-3	0.047349	53456.97	1133.7	17626.2	194.7	372265.5	8.99	6.04	2445.3	484.41	68.61	5.16	0.37	1613.10	10.78	1.51	424.96
15SB-2Aa-1	0.232924	46307.65	4590.4	68501.0	1284.8	294091.4	83.81	10.90	8456.7	899.27	43.26	6.54	1.59	1769.75	17.53	1.33	675.63
15SB-2Aa-2	0.451157	21914.43	2635.6	107974.2	456.4	239327.6	124.32	18.37	7825.4	494.76	114.29	11.31	1.24	1900.18	22.83	3.10	801.19
15SB-2Aa-3	0.137689	8735.675	4287.3	44243.9	1620.7	321331.9	53.30	26.96	14074.6	756.44	249.89	59.06	4.25	1232.86	14.25	10.29	411.53
15SB-2Aa-4	0.457366	39851.92	4473.7	108343.0	1141.4	236884.6	119.58	18.34	6410.1	378.14	78.07	10.99	2.30	2330.55	16.60	12.18	996.59
15SB-2Aa-5	0.440846	31363.96	2341.3	106863.6	296.4	242405.9	121.23	13.83	7304.4	445.16	41.09	6.09	0.74	2022.32	24.10	4.49	761.91
15SB-2A-1	0.396876	25173.39	3860.1	98075.4	1135.0	247118.5	115.16	80.40	12404.2	455.06	259.28	20.36	1.37	1950.83	14.33	5.71	857.76
15SB-2A-2	0.327842	48638.74	3108.0	88811.9	599.6	270898.5	102.62	13.72	5495.0	447.04	75.38	10.65	1.22	1999.70	22.55	2.52	701.30
15SB-2A-3	0.438693	47417.99	7215.0	104912.0	2041.4	239146.9	112.44	20.83	4919.8	327.20	140.46	13.33	2.00	2619.77	17.22	3.43	1284.77
15SB-2A-4	0.38403	41124.48	6167.2	96051.0	2282.2	250112.9	119.00	18.93	8931.5	549.69	129.11	12.51	2.90	2165.19	21.05	3.10	889.63
15SB-2A-5	0.354373	48500.84	19349.1	89187.9	513.9	251678.2	103.27	11.44	6261.9	455.76	53.06	6.00	1.45	1800.80	13.68	1.82	633.02
SB-2A6	0.413196	25819.56	2869.2	101140.5	679.2	244776.3	118.85	19.26	12103.5	615.52	106.47	11.99	1.58	1842.95	14.57	3.34	662.08
SB-5A1	0.194235	34290.3	2888.3	60043.0	610.9	309124.7	46.32	13.78	7162.3	628.65	72.11	9.55	1.79	1958.10	25.57	3.06	1069.80

39 La [ppb]	140 Ce [ppb]	141 Pr [ppb]	146 Nd [ppb]	147 Sm [ppb]	153 Eu [ppb]	157 Gd [ppb]	163 Dy [ppb]	165 Ho [ppb]	166 Er [ppb]	169 Tm [ppb]	172 Yb [ppb]	175 Lu [ppb]	208 Pb [ppb]	238 U[ppb]
2.19	8.30	0.85	3.91	1.03	0.38	1.22	1.76	0.43	1.40	0.22	1.49	5.93	97.54	3.72
4.20	12.89	1.75	8.31	2.09	0.66	2.45	2.92	0.66	1.99	0.30	1.89	6.40	52.41	3.18
3.89	14.97	1.51	6.91	1.70	0.50	2.06	2.31	0.51	1.70	0.25	1.74	11.18	87.99	3.22
7.47	20.30	2.61	12.07	3.03	0.80	3.17	2.96	0.62	1.88	0.27	1.83	8.55	51.80	2.76
7.21	22.04	2.15	9.09	1.96	0.59	2.14	1.88	0.42	1.21	0.18	1.21	10.56	45.65	12.48
11.42	33.58	3.25	14.32	3.18	0.85	3.49	3.25	0.71	2.26	0.34	2.24	7.84	74.78	21.65
0.88	2.04	0.22	0.90	0.19	0.16	0.20	0.18	0.04	0.12	0.02	0.13	5.77	28.38	0.66
8.16	23.13	2.79	12.28	2.75	0.74	3.11	3.21	0.72	2.24	0.32	2.18	7.79	89.30	7.49
6.30	18.47	2.32	10.85	2.49	0.71	2.99	3.22	0.73	2.27	0.34	2.32	7.00	49.08	6.86
9.87	24.60	3.28	14.62	3.28	0.85	3.58	3.46	0.76	2.26	0.33	2.16	6.73	61.87	6.72
5.31	14.51	1.88	8.62	1.99	0.58	2.33	2.57	0.59	1.80	0.25	1.69	13.98	167.46	4.79
3.03	9.78	1.14	5.46	1.39	0.47	1.73	2.22	0.53	1.72	0.27	1.79	4.78	52.20	6.68
3.79	9.88	1.27	5.88	1.46	0.44	1.74	2.10	0.49	1.53	0.23	1.63	6.50	26.08	5.15
4.42	13.76	1.64	7.70	1.79	0.59	2.19	2.77	0.66	2.09	0.31	2.16	5.85	46.85	5.26
8.84	23.71	2.78	12.16	2.60	0.74	2.96	2.45	0.51	1.52	0.24	1.56	16.86	230.40	4.16
4.78	13.30	1.46	6.49	1.60	0.57	1.78	1.79	0.43	1.43	0.21	1.63	17.34	99.22	7.08
5.90	14.97	1.79	7.88	1.76	0.50	1.82	1.64	0.35	1.06	0.16	1.10	6.70	25.58	4.07
5.98	15.96	1.83	8.05	1.86	0.55	2.00	1.91	0.42	1.35	0.21	1.46	11.88	199.92	5.52
4.54	15.67	1.60	7.66	1.81	0.59	2.06	1.98	0.44	1.38	0.21	1.43	15.05	180.27	5.93
4.73	14.58	1.53	7.11	1.74	0.59	1.96	2.04	0.44	1.52	0.24	1.76	17.48	95.55	6.91
5.46	17.26	1.85	8.69	2.26	0.71	2.45	2.43	0.53	1.64	0.25	1.83	9.09	43.19	6.16
4.21	11.39	1.30	5.87	1.55	0.54	1.69	1.75	0.39	1.34	0.21	1.45	9.76	81.38	5.25
8.03	20.64	2.43	10.51	2.38	0.63	2.49	2.12	0.44	1.36	0.20	1.34	5.90	93.73	4.33
11.66	28.73	4.17	18.88	4.32	1.14	4.74	4.65	0.98	2.85	0.40	2.62	5.13	88.09	3.04
7.78	25.04	2.66	11.99	2.67	0.68	2.94	2.71	0.58	1.73	0.25	1.54	5.31	41.04	4.40
4.04	13.36	1.35	6.04	1.39	0.39	1.58	1.62	0.35	1.06	0.16	1.11	6.30	56.93	2.86
11.20	19.78	1.75	7.17	1.53	0.46	1.86	2.19	0.55	1.77	0.27	1.80	7.07	30.89	3.65
4.69	15.82	1.47	6.93	1.64	0.54	2.13	2.72	0.70	2.38	0.39	2.62	13.97	99.45	6.05
7.11	17.80	1.89	7.92	1.73	0.42	1.86	1.99	0.45	1.38	0.20	1.34	36.68	202.93	5.02
5.31	18.04	1.76	7.56	1.83	0.60	2.10	2.40	0.61	1.86	0.33	1.83	7.62	66.28	7.44
6.28	22.50	2.05	9.21	2.29	0.64	2.69	3.45	0.81	2.62	0.41	2.63	9.82	25.75	10.01
4.93	15.86	1.49	6.65	1.50	0.48	1.73	2.02	0.47	1.53	0.23	1.49	11.98	102.20	5.89
7.66	24.90	2.30	10.01	2.35	0.63	2.71	3.13	0.74	2.39	0.36	2.36	6.50	47.23	9.75
6.55	21.36	2.16	9.51	2.08	0.68	2.30	2.51	0.58	1.86	0.29	1.78	6.38	95.06	8.12
7.21	23.48	2.14	9.45	2.15	0.65	2.61	3.05	0.72	2.29	0.34	2.19	7.40	84.52	5.84
3.68	11.90	1.17	5.15	1.22	0.42	1.51	1.76	0.47	1.47	0.24	1.51	6.46	32.71	3.98
5.23	16.99	1.50	6.47	1.42	0.43	1.77	2.09	0.47	1.53	0.23	1.53	11.85	96.26	3.85
11.05	33.76	3.66	16.34	3.71	1.02	4.14	4.03	0.89	2.69	0.39	2.51	9.39	74.68	6.58

mple Numb	[Mg/Ca]	Sum ppb	23 Na. [ppm	24 Mg. [ppb]	39 K. [ppb]	43 Ca. [ppb]	51 V. [ppb]	52 Cr. [ppb	54 Fe. [ppb]	55 Mn [ppb]	64 Zn [ppb]	65 Cu [ppb]	85 Rb[ppb]	88 Sr [ppb]	89 Y [ppb]	95 Mo [ppb]	137 Ba[ppb]
C1-BRECC	0.176117	44230.04	749.7	54566.1	623.4	309828.3	54.79	12.52	16057.2	861.10	66.42	12.78	3.29	1677.54	29.21	1.35	653.95
C2-BC	0.150191	34159.41	890.1	48329.9	316.0	321790.0	33.27	9.61	12616.6	724.57	63.20	7.43	1.12	1945.89	31.50	1.48	652.16
C2-AC	0.076082	23443.28	1188.7	26842.8	419.2	352815.3	23.93	12.92	8691.8	631.31	91.85	10.02	1.18	2219.14	26.77	2.58	726.21
D1-SR	0.004602	35578.32	745.8	1800.3	358.7	391191.8	4.56	10.08	1536.1	399.41	82.32	8.35	1.42	2686.01	24.89	2.20	937.07
D1-BA	0.103944	36768.18	986.0	35338.6	411.7	339975.6	34.18	12.88	11102.2	608.06	79.78	8.26	1.45	2008.65	30.02	1.82	744.46
D1-BB	0.133293	31471.61	1347.9	43117.4	446.0	323478.6	43.99	240.36	16489.5	671.28	126.05	14.72	1.41	2003.74	29.76	33.56	756.03
D1-BRECC	0.202475	29934.42	1716.4	60725.6	664.6	299916.6	52.45	28.14	16381.5	896.15	78.31	10.26	3.04	1801.90	30.34	4.33	628.25
D2-AC	0.077686	40573.92	730.8	27414.8	225.5	352892.0	23.59	118.90	8405.5	576.55	66.61	8.96	0.48	2349.71	25.54	16.89	755.71
D2-BC	0.167673	29336.07	1368.7	52670.5	468.3	314127.2	34.50	16.46	13636.9	709.15	128.13	15.03	1.63	1974.33	28.11	3.32	678.41
A1-SR	0.005234	57748.17	597.0	2047.8	351.6	391231.4	4.59	20.68	1640.9	395.27	69.99	6.51	1.63	2539.69	29.59	1.65	836.26
A1-BA	0.092968	30851.99	1015.7	32044.4	426.3	344682.9	33.88	12.91	10575.0	551.70	95.40	9.98	1.77	2022.66	31.72	5.88	755.84
A1-BB	0.135462	29550.08	1266.3	43905.5	515.2	324116.9	47.05	17.61	15027.4	656.17	207.50	12.68	2.02	2044.95	32.99	5.63	747.44
A2-BC	0.106161	41626.19	1322.9	36051.8	394.9	339596.0	26.18	15.14	10315.8	657.52	144.08	13.82	1.23	1890.00	29.47	4.46	646.48
A2-AC	0.06562	16927.83	1498.3	23380.4	501.9	356298.6	24.60	20.13	9078.3	615.09	144.23	14.86	1.48	2136.22	26.62	7.69	782.07
B2-BC	0.141957	45174.99	861.3	45994.9	319.0	324005.5	29.51	11.78	13455.4	736.31	57.43	8.79	1.25	1973.41	29.79	2.53	632.09
B2-Ac	0.08691	30828.62	1231.1	28405.8	370.4	326840.9	26.02	10.74	32324.6	640.92	87.14	9.87	1.16	2091.91	27.06	3.91	709.38
B3-BC	0.134594	37975.38	985.3	44103.1	340.4	327675.1	32.22	12.09	12107.0	616.27	133.44	8.78	1.23	2001.26	29.69	2.89	684.30
B3-AC	0.083528	37746.52	785.8	29292.4	257.1	350690.0	25.70	12.77	8411.6	672.55	64.07	7.26	0.68	2158.89	27.47	3.02	694.92
C1-BA	0.105006	49984.29	711.6	35687.9	240.7	339863.9	31.59	8.90	11277.1	588.04	44.03	5.07	0.97	2058.80	32.25	1.75	727.99
C1-BB	0.122281	44490.03	971.4	40303.0	338.2	329593.4	39.15	10.33	14649.1	695.90	52.79	6.80	1.41	2298.09	39.81	1.72	776.63
C1-SR	0.007102	58110.36	736.7	2766.1	507.9	389473.8	5.81	32.94	1957.9	409.68	80.13	10.11	2.66	2663.80	27.12	3.21	910.16

39 La [ppb	140 Ce [ppb	141 Pr [ppb]	146 Nd [ppb	47 Sm [ppb	153 Eu [ppb	57 Gd [ppb	163 Dy [ppb	165 Ho [ppb	166 Er [ppb]	169 Tm [ppb	172 Yb [ppb	175 Lu [ppb	208 Pb [ppb	238 U[ppb]
20.38	44.44	4.94	19.94	4.17	1.01	4.73	4.41	0.96	2.86	0.41	2.61	7.46	61.08	4.23
22.63	50.90	5.06	19.89	4.11	1.05	4.87	4.81	1.03	3.20	0.47	3.01	9.69	50.30	3.60
27.04	56.91	5.36	20.47	3.77	0.96	4.50	4.25	0.87	2.69	0.38	2.35	14.12	82.11	2.50
37.20	72.04	7.58	27.75	4.70	1.12	5.08	4.05	0.80	2.39	0.36	2.37	9.52	75.03	2.75
22.99	46.15	5.38	21.13	4.37	1.07	4.97	4.70	0.98	2.98	0.44	2.92	9.10	75.02	4.64
21.72	46.88	5.33	21.24	4.41	1.09	4.93	4.66	0.99	3.02	0.43	2.79	10.54	108.97	4.55
22.64	46.02	5.43	21.91	4.49	1.10	5.04	4.63	1.03	3.11	0.44	2.67	10.79	57.88	3.43
26.87	57.40	5.40	19.99	3.86	0.93	4.35	3.97	0.86	2.57	0.36	2.35	8.24	43.32	2.81
24.02	54.10	5.32	20.80	4.24	0.98	4.73	4.40	0.93	2.87	0.41	2.71	11.18	101.71	4.08
32.23	62.12	6.73	25.92	4.96	1.18	5.44	4.72	0.97	2.78	0.39	2.54	6.04	54.14	2.92
21.57	44.70	5.27	22.00	4.68	1.14	5.21	5.13	1.08	3.27	0.48	3.09	11.02	89.09	4.89
21.04	45.10	5.29	22.46	4.79	1.20	5.37	5.23	1.13	3.43	0.48	3.06	11.37	116.44	4.59
21.05	47.65	4.83	19.62	4.24	1.03	4.73	4.66	1.04	3.02	0.44	2.79	8.16	123.93	3.89
32.26	67.31	6.28	23.20	4.42	0.97	4.69	4.19	0.92	2.64	0.38	2.51	19.73	123.18	2.97
21.72	51.66	5.02	20.88	4.40	1.05	5.04	4.71	1.05	3.01	0.45	2.71	7.44	48.95	4.10
28.99	61.28	5.83	22.04	4.24	0.99	4.71	4.29	0.94	2.75	0.39	2.43	10.90	72.82	2.90
20.88	48.67	4.87	19.74	4.12	1.03	4.81	4.75	1.02	3.06	0.46	2.93	8.90	67.96	4.25
26.54	55.78	5.31	20.73	4.06	0.96	4.46	4.27	0.95	2.75	0.40	2.50	8.98	50.93	2.62
20.44	44.88	5.15	21.88	4.72	1.14	5.24	5.03	1.13	3.25	0.47	2.95	6.94	50.86	4.85
26.39	57.87	6.74	28.56	6.15	1.43	6.59	6.41	1.39	4.13	0.56	3.40	7.76	43.47	4.51
35.68	71.19	7.46	28.63	5.06	1.14	5.41	4.41	0.90	2.60	0.37	2.52	5.92	65.52	3.10